Particle plasmon resonances in L-shaped gold nanoparticles

Hannu Husu,[1,*] Jouni Mäkitalo,[1] Janne Laukkanen,[2] Markku Kuittinen,[2] and Martti Kauranen[1]

[1]*Department of Physics, Optics Laboratory, Tampere University of Technology, P. O. Box 692, FI-33101 Tampere, Finland*
[2]*Department of Physics and Mathematics, University of Eastern Finland, P. O. Box 111, FI-80101 Joensuu, Finland*
**hannu.husu@tut.fi*

Abstract: We present an extensive experimental and theoretical study of the particle plasmon resonances of L-shaped gold nanoparticles. For the small characteristic size of the particles, we observe more higher-order resonances than previously from related shapes, and show that a short-wavelength resonance arises from the particle width and is not the suggested volume plasmon. We interpret the resonances through the local vector electric field in the structure and by fully taking into account the particle symmetry.

OCIS codes: (160.3900) Metals; (250.5403) Plasmonics; (310.6628) Subwavelength structures, nanostructures.

References and links

1. J.-J. Greffet, "Applied physics. Nanoantennas for light emission," Science **308**(5728), 1561–1563 (2005).
2. L. A. Sweatlock, S. A. Maier, H. A. Atwater, J. J. Penninkhof, and A. Polman, "Highly confined electromagnetic fields in arrays of strongly coupled Ag nanoparticles," Phys. Rev. B **71**(23), 235408 (2005).
3. V. M. Shalaev, W. Cai, U. K. Chettiar, H.-K. Yuan, A. K. Sarychev, V. P. Drachev, and A. V. Kildishev, "Negative index of refraction in optical metamaterials," Opt. Lett. **30**(24), 3356–3358 (2005).
4. L. Novotny, and B. Hecht, *Principles of Nano-Optics* (Cambridge University Press, 2006).
5. B. Lamprecht, A. Leitner, and F. Aussenegg, "SHG studies of plasmon dephasing in nanoparticles," Appl. Phys. B **68**(3), 419–423 (1999).
6. B. Canfield, S. Kujala, K. Jefimovs, J. Turunen, and M. Kauranen, "Linear and nonlinear optical responses influenced by broken symmetry in an array of gold nanoparticles," Opt. Express **12**(22), 5418–5423 (2004).
7. B. K. Canfield, S. Kujala, K. Jefimovs, T. Vallius, J. Turunen, and M. Kauranen, "Polarization effects in the linear and nonlinear optical responses of gold nanoparticle arrays," J. Opt. A, Pure Appl. Opt. **7**(2), S110–S117 (2005).
8. M. Sukharev, J. Sung, K. G. Spears, and T. Seideman, "Optical properties of metal nanoparticles with no center of inversion symmetry: Observation of volume plasmons," Phys. Rev. B **76**(18), 184302 (2007).
9. Y. Jing, Z. Jia-Sen, W. Xiao-Fei, and G. Qi-Huang, "Resonant Modes of L-Shaped Gold Nanoparticles," Chin. Phys. Lett. **26**(6), 067802 (2009).
10. E. Tatartschuk, E. Shamonina, and L. Solymar, "Plasmonic excitations in metallic nanoparticles: resonances, dispersion characteristics and near-field patterns," Opt. Express **17**(10), 8447–8460 (2009).
11. C. Rockstuhl, F. Lederer, C. Etrich, T. Zentgraf, J. Kuhl, and H. Giessen, "On the reinterpretation of resonances in split-ring-resonators at normal incidence," Opt. Express **14**(19), 8827–8836 (2006).
12. T. D. Corrigan, P. W. Kolb, A. B. Sushkov, H. D. Drew, D. C. Schmadel, and R. J. Phaneuf, "Optical plasmonic resonances in split-ring resonator structures: an improved LC model," Opt. Express **16**(24), 19850–19864 (2008).
13. A. K. Sheridan, A. W. Clark, A. Glidle, J. M. Cooper, and D. R. S. Cumming, "Multiple plasmon resonances from gold nanostructures," Appl. Phys. Lett. **90**(14), 143105 (2007).
14. A. Vial, A.-S. Grimault, D. Macías, D. Barchiesi, and M. L. de la Chapelle, "Improved analytical fit of gold dispersion: Application to the modeling of extinction spectra with a finite-difference time-domain method," Phys. Rev. B **71**(8), 085416 (2005).
15. L. Novotny, "Effective wavelength scaling for optical antennas," Phys. Rev. Lett. **98**(26), 266802 (2007).
16. M. M. Miller, and A. A. Lazarides, "Sensitivity of metal nanoparticle surface plasmon resonance to the dielectric environment," J. Phys. Chem. B **109**(46), 21556–21565 (2005).

1. Introduction

Metal nanostructures offer the possibility to control light in the nanoscale. Most of their possible applications, like nanoantennas [1], nanoscale waveguides [2], and metamaterials [3],

#129400 - $15.00 USD Received 1 Jun 2010; revised 1 Jul 2010; accepted 5 Jul 2010; published 22 Jul 2010

are based on the nanostructures' ability to confine strong local electromagnetic fields. Particle plasmon resonances are collective oscillations of the conduction electrons of the nanoparticle, which can hugely enhance the local electric fields [4]. When measuring the extinction spectrum of such a structure, one may observe several different plasmon resonances which are not well understood so far, except for the most basic particle shapes.

In this paper, we consider the plasmon resonances of L-shaped nanoparticles. The L-shape is the basic noncentrosymmetric shape, also used in second-order nonlinear investigations [5–7]. The resonances of L-shaped particles have been addressed [8–10], but the explanations are incomplete and partly different from our interpretations. Sukharev et al. [8] treated the fundamental resonances properly, but did not observe any higher-order resonances. A short-wavelength resonance was interpreted as a volume plasmon, although they should not be excitable with light. Jing et al. [9] explain the fundamental resonances and provide experimental evidence of higher-order resonances, which, however, are not further explained. Tatartschuk et al. [10] consider, only computationally, several different particle shapes, including the L-shape where they find three resonances, but do not assign them in detail.

Discussions partly related to the present work have earlier been presented for U-shaped and crescent-shaped split-ring resonators [11–13]. Several resonances were computationally predicted [11] and some of them experimentally observed [12,13]. A short-wavelength resonance was interpreted as arising from the width of the structure, because of its insensitivity to other structural dimensions. However, more detailed information to support this interpretation, such as local field calculations, was not presented [11,13].

The differences in our and earlier interpretations are related to the various approaches taken to treat the optical properties of metal nanostructures. To simplify the treatment, it is common to adapt methods from the basic electric circuit theory, where the electric field of the incoming light simply induces a current along a structural feature. However, this approach does not properly account for the importance of symmetry in the optical response of the structures. More specifically, the L, U and crescent shapes are dichroic, i.e., their resonances depend on polarization. It is therefore essential to choose the proper polarization to excite the desired resonance mode and to understand its origin. This issue is somewhat less of a problem for the U-shape, whose eigenpolarizations are along the sides and the bottom of the U. Therefore, for the incoming field along the feature lines, only one eigenpolarization is excited. For the L-shape, however, the eigenpolarizations are rotated by 45° from the arm directions. Incident field along an arm therefore excites both eigenpolarizations simultaneously, which complicates the interpretation of the results and has not always been taken into account [10].

In the present work, we thus give a comprehensive analysis of the multiple resonances that may occur in the L-shaped gold nanoparticles, which takes properly into account the influence of symmetry. For the characteristic small size of the particles, we observe more higher-order resonances than previously for any shape and explain the features by detailed theoretical calculations. We also show that a short-wavelength resonance is not a volume plasmon but arises from the arm width of the particles.

2. Experiments

Arrays of gold nanoparticles were fabricated by electron-beam lithography and lift-off techniques. The thickness of the particles is fixed to 20 nm and the array period is 500 nm. The nanoparticles are placed on a silica substrate and they are covered with a 20 nm-thick protective layer of silica. Between the substrate and the nanoparticles, there is a 5 nm-thick adhesion layer of chromium. We consider bars and more complex L-shaped nanoparticles. The bar is a highly symmetric, but nevertheless dichroic, shape (Fig. 1a, inset), which is used as a reference to interpret some of the resonances of the L-shape. The L-shape is still a relatively simple structure but has lower symmetry (Fig. 1b, inset), and thus has multiple resonance modes. The eigenpolarizations of the bars are labeled *x* and *y*, whereas those of the L-shape are labeled *a* and *b*, and are rotated by 45° from the direction of the arms of the L-shape. The *b* direction is a mirror plane of the L-shape.

#129400 - $15.00 USD Received 1 Jun 2010; revised 1 Jul 2010; accepted 5 Jul 2010; published 22 Jul 2010

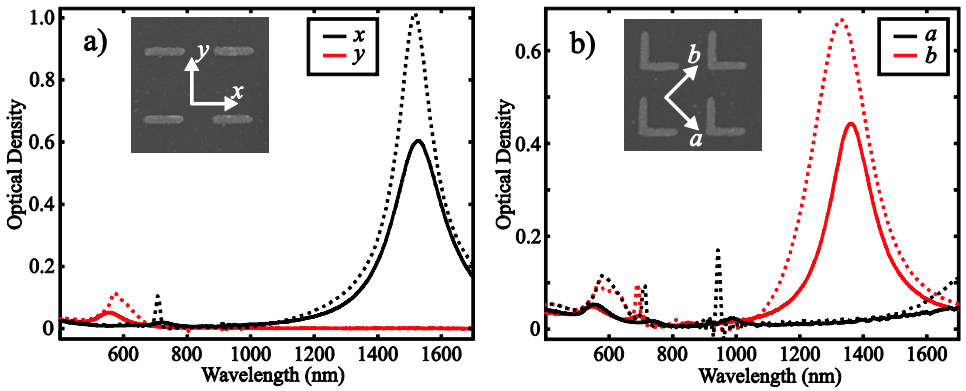

Fig. 1. The extinction spectra of an array of a) bars (length 300 nm, width 50 nm) for *x* and *y* polarization, and b) L-particles (arm length 300 nm, arm width 50 nm) for *a* and *b* polarization, which are the eigenpolarizations of the structure along the mirror plane and perpendicular to it. Solid lines are measured spectra and dashed lines are calculated. Insets: Scanning electron microscope images of bars and L-particles, and the coordinate systems.

The extinction spectra of the samples were measured using two fiber coupled spectrometers (Avantes AvaSpec-2048 and Avantes NIR-128) to cover a spectral range from 400 to 1700 nm (Fig. 1, solid lines). The data are combined at 910 nm, around which both spectrometers have reduced sensitivity, causing some additional noise in the data. The light source was a tungsten halogen lamp (StellarNet SL1). Light from the fiber output was collimated using a microscope objective and the polarization state was selected with a high-quality broadband calcite polarizer. A pinhole was used in front of the sample to illuminate only the sample area. The excitation was performed at normal incidence. The transmitted light was focused to the spectrometer pick-up fiber using a microscope objective.

We have also calculated the extinction spectra of the arrays to compare with the measured data (Fig. 1, dashed lines). Our code is based on a full three-dimensional finite-difference time-domain (FDTD) solution of Maxwell's equations. For the gold permittivity, we use the Drude-Lorentz model fitted to the measured values, which works well also at shorter wavelengths [14]. In the calculations, the corners of the bars and L-shapes are rounded.

Figure 1a shows the extinction spectra of 300 nm long bars in a rectangular array for *x* and *y* polarizations. The locations of the spectral peaks are related to the dimensions of the bar, i.e., the length and the width of the bar. Note, however, that the resonance wavelengths are not related to the bar length in such a simple way as in traditional antenna theory [15]. The large peak at 1500 nm is the fundamental resonance for *x* polarization. A smaller peak at 700 nm for *x* polarization is a higher-order mode, which is observed both experimentally and theoretically. The *y*-polarized spectra corresponding to the width of the bar show a weak resonance at 550 nm observed both in the measured and calculated spectra.

Figure 1b shows the extinction spectra of the L-shape for its eigenpolarizations. The fundamental resonance for *a*-polarized light is beyond the range of our spectrometer but its tail is observed. The fundamental resonance for *b* polarization is at 1350 nm. Several higher-order resonances are also observed. For *a* polarization, they occur at 980 nm and 740 nm, and for *b* polarization at 850 nm (very broad) and 700 nm. All the higher-order resonances are observed also experimentally although the peak locations do not match perfectly. Both polarizations show a resonance at about 560 nm, both in the measured and calculated spectra, which is very close to the *y*-polarized resonance of the bar with the same width (Fig. 1a). This already suggests that the resonance is related to the arm width of the L-shape.

We note that it is a significant achievement that all the resonances of the calculated spectra are observed also experimentally. For L-shaped particles only few of these resonances have been seen earlier. Also, for other shapes with similar characteristic sizes, so many higher-order resonances have not been observed. For larger sizes the higher-order resonances would be stronger and more easily recognized, but at longer infrared wavelengths.

#129400 - $15.00 USD Received 1 Jun 2010; revised 1 Jul 2010; accepted 5 Jul 2010; published 22 Jul 2010

3. Resonances

In order to explain the resonances in more detail, we will next look at the situation on the level of individual particles. In the previous section, we considered arrays of particles as single particles cannot be easily measured. It is known that the array and also the dielectric environment affect the spectrum [7,16]. We have performed additional calculations to verify that the substrate clearly shifts the resonance but that the array has only a very small effect. The calculations also show that the presence of the substrate or a homogeneous dielectric environment only influences the locations of the resonances but not their character. We therefore consider from now on single particles in vacuum, which represents the simplest possible situation and results in the highest quality of the calculated spectra.

To explain the resonances, the most common way is to look at the distribution of the local electric field, either the total field or its certain component. In addition to the total electric field magnitude we also use information about its direction. Our results thus display the total vectorial electric fields, where arrows show the direction of the electric field and color illustrates the magnitude. The snapshot of the field oscillation is taken at the moment when the strongest fields occur at the ends of the structure. These calculations are also performed using FDTD and the fields are shown in the middle layer of the structure. From the field distribution it is easy to recognize the sources and sinks, which are the poles of the resonance, and thus, we can identify the type of the resonance and to which part of the structure it is connected.

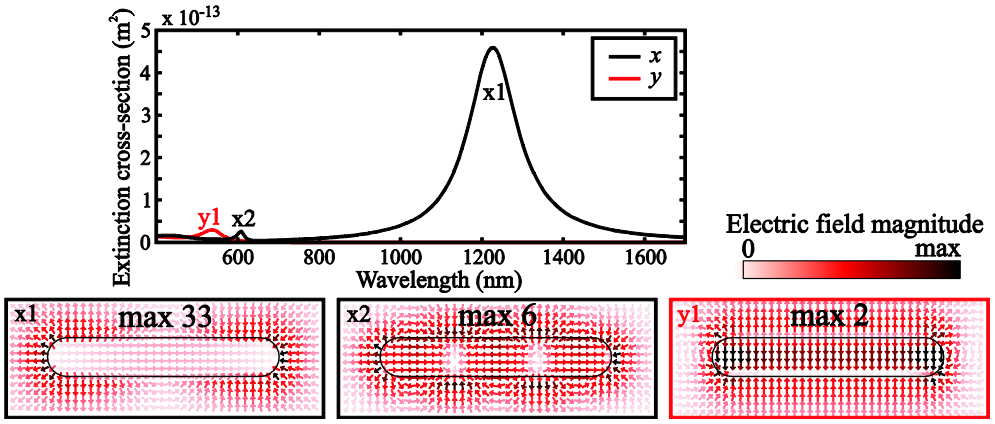

Fig. 2. Calculated extinction cross-section spectra of a single bar for *x* and *y* polarization. Vector field presentation of the local electric field at the fundamental resonance for *x* polarization (x1), higher-order resonance for *x* polarization (x2) and the resonance for *y* polarization (y1). The distributions are normalized to the maximum of each plot separately.

We first consider the resonances of a bar. The calculated extinction cross-section spectra are presented in Fig. 2 for *x* and *y* polarizations. The resonance peaks are shifted compared to Fig. 1a due to the absence of the dielectric environment, but the corresponding peaks can be found in both spectra. The fundamental resonance for *x* polarization is found at 1230 nm and its field distribution has poles at the ends of the bar (Fig. 2(x1)). The resonance at 610 nm is a higher-order resonance, which is evident from the vector field distribution (Fig. 2(x2)). This higher-order mode has four poles instead of three as one could guess. A resonance with three poles would have the same phase for the fields at the ends of the bar, and thus, it cannot be excited by the incoming light [10]. The resonance for *y* polarization is at 540 nm, which clearly corresponds to the width of the bar (Fig. 2(y1)).

#129400 - $15.00 USD Received 1 Jun 2010; revised 1 Jul 2010; accepted 5 Jul 2010; published 22 Jul 2010

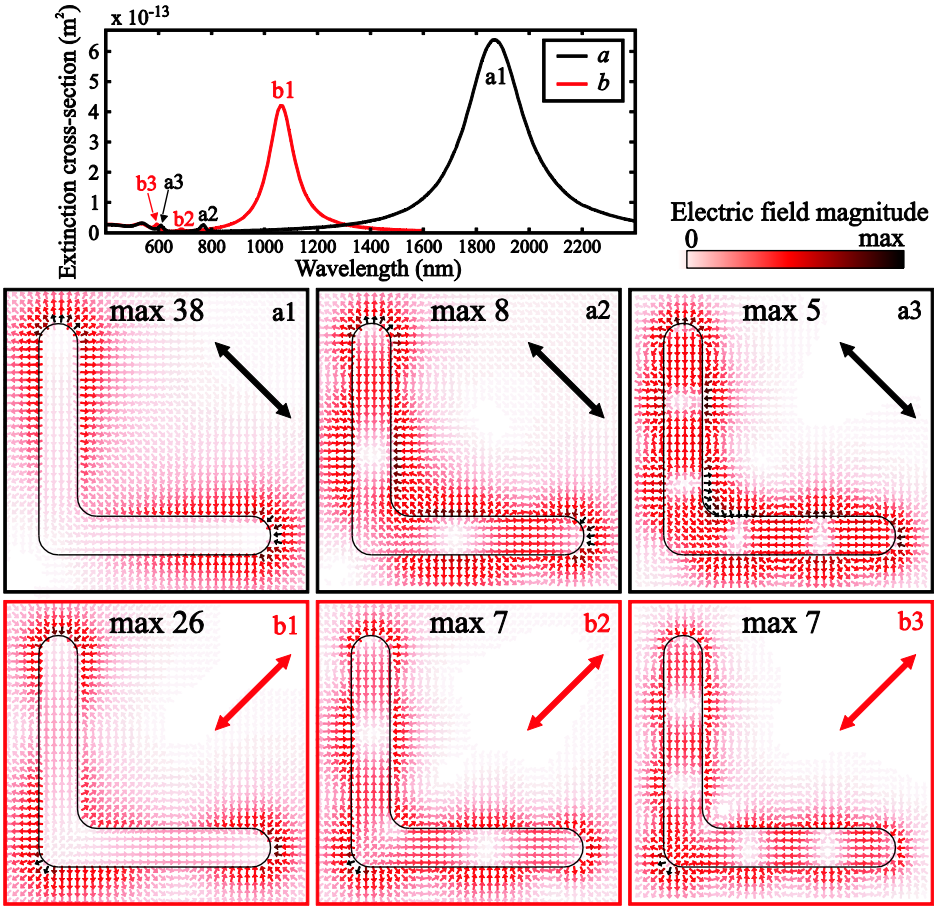

Fig. 3. Calculated extinction cross-section spectra of a single L-shaped nanoparticle (arm length 300 nm, arm width 50 nm) for *a* and *b* polarization. Vector field presentation of the local electric field for *a* and *b* polarization at the fundamental resonance (1) and at the higher-order resonances (2, 3). The distributions are normalized to the maximum of each plot separately.

The calculated extinction cross-section spectra of an L-shaped nanoparticle in vacuum are shown in Fig. 3. The fundamental resonance for *a* polarization is found at 1870 nm and it corresponds to oscillation over the whole length of the L-shape (Fig. 3(a1)). Note that, unlike earlier interpretations [10], the resonance cannot be considered simply as a resonance of a bent bar, because the resonance of a bar of 550 nm equivalent length is shifted 100 nm to longer wavelengths. Also, because of its different symmetry, the L-shape has additional resonances, which are not even observed in a bar. The higher-order resonance at 770 nm corresponds to a more complex local-field distribution with four poles distributed to both arms (Fig. 3(a2)). A third resonance at 610 nm is an even higher-order resonance with six poles (Fig. 3(a3)). A short wavelength resonance for *a*-polarized light is at 540 nm and based on the vector field distribution it is related to the width of the arms (Fig. 4(a)). Also, the resonance wavelength is very close to that of the *y* resonance of a bar. In all these cases, the ends of the arms are in opposite phase, and thus the resonances couple with the incoming *a*-polarized electric field.

The spectrum for *b* polarization has similar features (Fig. 3). The fundamental resonance at 1060 nm corresponds to oscillation along the arms of L-shape and has three poles (Fig. 3(b1)). The higher-order resonance at 690 nm is more complicated with five poles (Fig. 3(b2)). A third resonance at 590 nm has seven poles as expected (Fig. 3(b3)). A short

#129400 - $15.00 USD Received 1 Jun 2010; revised 1 Jul 2010; accepted 5 Jul 2010; published 22 Jul 2010

wavelength resonance at 540 nm is again related to the width of the arms (Fig. 4(b)). For these resonances the ends of the arms are in phase, and therefore they couple with *b* polarization.

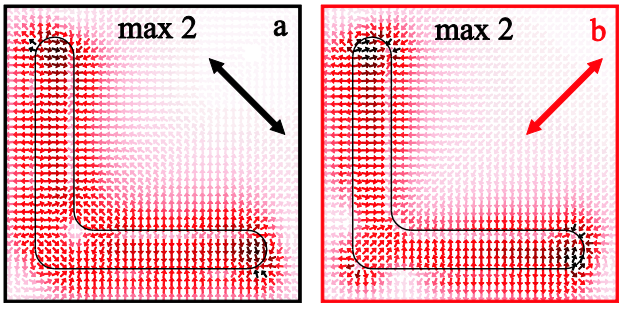

Fig. 4. Local vector electric field distributions at the arm-width-related resonances at 540 nm for *a* and *b* polarization. (Media 1)

We note that both arm-width-related resonances (Fig. 4) have some additional features in the electric-field distribution. This is because the distributions must also conform to the symmetry of the L-shape, which is lower than that of the bar. Furthermore, the arm-width-related resonances partly overlap with the higher-order particle resonances, and they may thus interfere. The most interesting consequence of this is that when looking at the dynamics of the *b* resonance at 540 nm (Media1), the local fields seem to propagate along the arms instead of just oscillating back and forth. Note that the incident wave is applied at normal incidence and this result can thus not be explained by any in-plane wave vector component.

4. Discussion

We have investigated the particle plasmon resonances of L-shaped gold nanoparticles. In the experimental extinction spectra of an array of such particles, we have observed the highest number of higher-order resonances to date, which are predicted by FDTD computations. To explain the resonances, we considered the local vectorial electric field in the structure, which clearly shows the types of different resonances and to which part of the structure a certain resonance is related. The resonances are strongly influenced by the symmetry of the structure. This gives rise to distinct sets of resonances of different orders for the two eigenpolarizations, which depend on the particle size. The effect of symmetry is particularly evident for the fundamental plasmonic modes for the two eigenpolarizations. Neither of these resonances can be considered as a resonance of a bent bar, because they occur at wavelengths shorter than the resonance of a bar with reasonable equivalent length. Additional short-wavelength resonances associated with the width of the particles were also observed.

The arm-width-related resonance has earlier been associated with a volume plasmon, as the electric field extends through the particle [8]. It was suggested that because of the asymmetry of the L-shape, a volume plasmon can be excited although it should be forbidden. However, at short wavelengths down to 490 nm, the skin depth of gold increases, and thus, the electric field penetrates deeper into the structure. The same effect can be seen also in the width-related resonance of a bar. Also, all the higher-order modes always have a strong electric field inside the particle. Thus, the arm-width-related resonance is a particle plasmon and does not anyhow violate the basic rules of plasmons.

Acknowledgments

We acknowledge the support by the Academy of Finland (320002, 310007) and by the Nanophotonics Program of the Ministry of Education of Finland. HH acknowledges support from the Graduate School of Tampere University of Technology and the Finnish Foundation for Technology Promotion. JL acknowledges support from Emil Aaltonen Foundation. Fruitful discussions with Lauri Kettunen and Saku Suuriniemi are greatly appreciated. We also thank Kalle Koskinen for help in the measurements.

#129400 - $15.00 USD Received 1 Jun 2010; revised 1 Jul 2010; accepted 5 Jul 2010; published 22 Jul 2010